The Sixteenth International Congress on Sound and Vibration
Kraków, 5-9 July 2009

SINGULAR FEATURES OF TRAVELING WAVE PROPAGATION IN ROTATING ELASTIC BODIES OF REVOLUTION IN FRICTIONAL CONTACT

Oleg N. Kirillov

Dynamics and Vibration Group, Department of Mechanical Engineering
Technische Universität Darmstadt, Hochschulstr. 1, D-64289 Darmstadt, Germany
email: kirillov@dyn.tu-darmstadt.de

Electromagnetic and acoustic wave propagation in the stationary anisotropic media, such as optically anisotropic crystals that are both absorbing and chiral, is accompanied by the polarization singularities among which the singular axes are the most prominent [8, 11]. These are degeneracies where the two refractive indices are equal and that for a transparent non-chiral crystal condense pairwise onto the optic axes. The present work reveals these singularities in case of the traveling bending waves that propagate in the rotating continua. We consider an axi-symmetric rotor perturbed by dissipative, conservative, and non-conservative positional forces originated at the contact with the anisotropic stator. The Campbell diagram of the unperturbed system is a mesh-like structure in the frequency-speed plane with double eigenfrequencies at the nodes. Computing sensitivities of the doublets we find that selection of the unstable modes that cause self-excited vibrations in the subcritical speed range is governed by the exceptional points at the corners of the singular eigenvalue surfaces - "double coffee filter" [12] and "viaduct" - that are sharply associated with the crossings of the unperturbed Campbell diagram with the definite Krein signature. As a mechanical example a rotating circular string passing through the eyelet is studied in detail.

1. Introduction

Bending waves propagate in the circumferential direction of an elastic body of revolution rotating about its axis of symmetry [1, 5, 9, 16]. The frequencies of the waves plotted against the rotational speed are referred to as *the Campbell diagram* [1, 16]. Since the spectrum of a perfect rotationally symmetric rotor at standstill has infinitely many double semi-simple eigenvalues - *the doublet modes* - the Campbell diagram contains the eigenvalue branches originated after the splitting of the doublets by the gyroscopic forces. The branches correspond to simple pure imaginary eigenvalues and intersect each other forming a *spectral mesh* [20] in the frequency-speed plane with the double eigenfrequencies at the nodes. Dissipative, conservative, and non-conservative perturbations of the axially symmetric rotor, caused by its contact with the anisotropic stator, generically untwist the spectral mesh of pure imaginary eigenvalues of the Campbell diagram into the separate branches of complex eigenvalues in the $(\Omega, \mathrm{Im}\lambda, \mathrm{Re}\lambda)$-space. This complicated behavior is difficult to predict [1, 4, 5, 6, 7, 9, 10, 14, 15, 16, 21]. The present work reveals that the untwisting of the Campbell diagrams is determined by a limited number of singular eigenvalue surfaces.

2. A model of a weakly anisotropic rotor system

An axially symmetric rotor with an anisotropic stator as well as an asymmetric rotor with an isotropic stator are autonomous non-conservative gyroscopic systems [16]. Neglecting the centrifugal stiffness without loss of generality, we consider the anisotropic rotor system

$$\ddot{\mathbf{x}} + (2\Omega\mathbf{G} + \delta\mathbf{D})\dot{\mathbf{x}} + (\mathbf{P} + \Omega^2\mathbf{G}^2 + \kappa\mathbf{K} + \nu\mathbf{N})\mathbf{x} = 0, \;\; \mathbf{x} = \mathbb{R}^{2n} \tag{1}$$

which is a perturbation of the isotropic one

$$\ddot{\mathbf{x}} + 2\Omega\mathbf{G}\dot{\mathbf{x}} + (\mathbf{P} + \Omega^2\mathbf{G}^2)\mathbf{x} = 0, \tag{2}$$

where $\mathbf{P} = \mathrm{diag}(\omega_1^2, \omega_1^2, \omega_2^2, \omega_2^2, \ldots, \omega_n^2, \omega_n^2)$ and $\mathbf{G} = -\mathbf{G}^T$ are the stiffness and gyroscopic matrices,

$$\mathbf{G} = \mathrm{blockdiag}(\mathbf{J}, 2\mathbf{J}, \ldots, n\mathbf{J}), \quad \mathbf{J} = \begin{pmatrix} 0 & -1 \\ 1 & 0 \end{pmatrix}. \tag{3}$$

The matrices of damping, $\mathbf{D} = \mathbf{D}^\mathbf{T}$, stiffness, $\mathbf{K} = \mathbf{K}^\mathbf{T}$, and circulatory forces, $\mathbf{N} = -\mathbf{N}^\mathbf{T}$, can depend on the rotational speed Ω. The perturbation is controlled by the parameters δ, κ, and ν.

At $\Omega = 0$ the eigenvalues $\pm i\omega_s$, $\omega_s > 0$, of the isotropic rotor (2) are double semi-simple. Substituting $\mathbf{x} = \mathbf{u}\exp(\lambda t)$ into (2), we arrive at the eigenvalue problem for the operator $\mathbf{L}_0$

$$\mathbf{L}_0(\Omega)\mathbf{u} := (\mathbf{I}\lambda^2 + 2\Omega\mathbf{G}\lambda + \mathbf{P} + \Omega^2\mathbf{G}^2)\mathbf{u} = 0. \tag{4}$$

The eigenvalues of $\mathbf{L}_0$ are found in the explicit form

$$\lambda_s^+ = i\omega_s + is\Omega, \quad \overline{\lambda_s^-} = -i\omega_s + is\Omega, \quad \lambda_s^- = i\omega_s - is\Omega, \quad \overline{\lambda_s^+} = -i\omega_s - is\Omega, \tag{5}$$

where the overbar denotes complex conjugate. The eigenvectors of λ_s^+ and $\overline{\lambda_s^-}$ are

$$\mathbf{u}_1^+ = (-i, 1, 0, 0, \ldots, 0, 0)^T, \; \ldots, \; \mathbf{u}_n^+ = (0, 0, \ldots, 0, 0, -i, 1)^T, \tag{6}$$

where the imaginary unit holds the $(2s-1)$st position in the vector $\mathbf{u}_s^+$. The eigenvectors, corresponding to the eigenvalues λ_s^- and $\overline{\lambda_s^+}$, are simply $\mathbf{u}_s^- = \overline{\mathbf{u}_s^+}$.

For $\Omega > 0$, simple eigenvalues λ_s^+ and λ_s^- correspond to the forward and backward traveling waves, respectively. At the angular velocity $\Omega_s^{cr} = \omega_s/s$ the frequency of the sth backward traveling wave vanishes to zero, so that the wave remains stationary in the non-rotating frame. We assume further in the text that $\omega_{s+1} - \omega_s \geq \Omega_s^{cr}$, which implies the existence of the minimal *critical* speed $\Omega_{cr} = \Omega_1^{cr} = \omega_1$. When $\Omega > \omega_1$, some backward waves, corresponding to the eigenvalues $\overline{\lambda_s^-}$, travel slower than the disc rotation speed and appear to be traveling forward (reflected waves).

3. Perturbation of the doublets

Introducing the indices $\alpha, \beta, \varepsilon, \sigma = \pm 1$ we find that two branches of the spectral mesh $\lambda_s^\varepsilon = i\alpha\omega_s + i\varepsilon s\Omega$ and $\lambda_t^\sigma = i\beta\omega_t + i\sigma t\Omega$ cross each other at $\Omega = \Omega_0$ with the origination of the double semi-simple eigenvalue $\lambda_0 = i\omega_0$ with two linearly-independent eigenvectors $\mathbf{u}_s^\varepsilon$, $\mathbf{u}_t^\sigma$, where

$$\Omega_0 = \frac{\alpha\omega_s - \beta\omega_t}{\sigma t - \varepsilon s}, \quad \omega_0 = \frac{\alpha\sigma\omega_s t - \beta\varepsilon\omega_t s}{\sigma t - \varepsilon s}. \tag{7}$$

Let $\mathbf{M}$ be one of the matrices $\mathbf{D}, \mathbf{K}$, or $\mathbf{N}$. In the following, we decompose the matrix $\mathbf{M} \in \mathbb{R}^{2n\times 2n}$ into n^2 blocks $\mathbf{M}_{st} \in \mathbb{R}^{2\times 2}$, where $s, t = 1, 2, \ldots, n$

$$\mathbf{M}_{st} = \begin{pmatrix} m_{2s-1,2t-1} & m_{2s-1,2t} \\ m_{2s,2t-1} & m_{2s,2t} \end{pmatrix}. \tag{8}$$

We consider a small perturbation of the matrix operator of the isotropic rotor $\mathbf{L}_0(\Omega) + \Delta\mathbf{L}(\Omega)$, where $\Delta\mathbf{L}(\Omega) = \delta\lambda\mathbf{D} + \kappa\mathbf{K} + \nu\mathbf{N} \sim \tau$ with $\tau = \|\Delta\mathbf{L}(\Omega_0)\|$ [13].

The real and imaginary parts of the sensitivity of the doublet $\lambda_0 = i\omega_0$ at the crossing (7) are

$$\mathrm{Re}\lambda = -\frac{1}{8}\left(\frac{\mathrm{Im}A_1}{\alpha\omega_s} + \frac{\mathrm{Im}B_1}{\beta\omega_t}\right) \pm \sqrt{\frac{|c| - \mathrm{Re}c}{2}},$$

$$\mathrm{Im}\lambda = \omega_0 + \frac{\Delta\Omega}{2}(s\varepsilon + t\sigma) + \frac{\kappa}{8}\left(\frac{\mathrm{tr}\mathbf{K}_{ss}}{\alpha\omega_s} + \frac{\mathrm{tr}\mathbf{K}_{tt}}{\beta\omega_t}\right) \pm \sqrt{\frac{|c| + \mathrm{Re}c}{2}}, \tag{9}$$

where $c = \mathrm{Re}c + i\,\mathrm{Im}c$ with

$$\mathrm{Im}c = \frac{\alpha\omega_t \mathrm{Im}A_1 - \beta\omega_s \mathrm{Im}B_1}{8\omega_s\omega_t}(s\varepsilon - t\sigma)\Delta\Omega$$
$$+ \kappa\frac{(\alpha\omega_s \mathrm{tr}\mathbf{K}_{tt} - \beta\omega_t \mathrm{tr}\mathbf{K}_{ss})(\alpha\omega_s \mathrm{Im}B_1 - \beta\omega_t \mathrm{Im}A_1)}{32\omega_s^2\omega_t^2} - \alpha\beta\kappa\frac{\mathrm{Re}A_2 \mathrm{tr}\mathbf{K}_{st}\mathbf{J}_{\varepsilon\sigma} - \mathrm{Re}B_2 \mathrm{tr}\mathbf{K}_{st}\mathbf{I}_{\varepsilon\sigma}}{8\omega_s\omega_t},$$

$$\mathrm{Re}c = \left(\frac{t\sigma - s\varepsilon}{2}\Delta\Omega + \kappa\frac{\beta\omega_s \mathrm{tr}\mathbf{K}_{tt} - \alpha\omega_t \mathrm{tr}\mathbf{K}_{ss}}{8\omega_s\omega_t}\right)^2 + \alpha\beta\frac{(\mathrm{tr}\mathbf{K}_{st}\mathbf{J}_{\varepsilon\sigma})^2 + (\mathrm{tr}\mathbf{K}_{st}\mathbf{I}_{\varepsilon\sigma})^2}{16\omega_s\omega_t}\kappa^2$$
$$- \frac{(\alpha\omega_s \mathrm{Im}B_1 - \beta\omega_t \mathrm{Im}A_1)^2 + 4\alpha\beta\omega_s\omega_t((\mathrm{Re}A_2)^2 + (\mathrm{Re}B_2)^2)}{64\omega_s^2\omega_t^2}. \tag{10}$$

The coefficients A_1, A_2 and B_1, B_2 depend only on those entries of the matrices $\mathbf{D}$, $\mathbf{K}$, and $\mathbf{N}$ that belong to the four 2×2 blocks (8) with the indices s and t

$$A_1 = \delta\lambda_0 \mathrm{tr}\mathbf{D}_{ss} + \kappa\mathrm{tr}\mathbf{K}_{ss} + \varepsilon 2i\nu n_{2s-1,2s}, \quad A_2 = \sigma\nu\mathrm{tr}\mathbf{N}_{st}\mathbf{I}_{\varepsilon\sigma} + i(\delta\lambda_0 \mathrm{tr}\mathbf{D}_{st}\mathbf{J}_{\varepsilon\sigma} + \kappa\mathrm{tr}\mathbf{K}_{st}\mathbf{J}_{\varepsilon\sigma}),$$
$$B_1 = \delta\lambda_0 \mathrm{tr}\mathbf{D}_{tt} + \kappa\mathrm{tr}\mathbf{K}_{tt} + \sigma 2i\nu n_{2t-1,2t}, \quad B_2 = \sigma\nu\mathrm{tr}\mathbf{N}_{st}\mathbf{J}_{\varepsilon\sigma} - i(\delta\lambda_0 \mathrm{tr}\mathbf{D}_{st}\mathbf{I}_{\varepsilon\sigma} + \kappa\mathrm{tr}\mathbf{K}_{st}\mathbf{I}_{\varepsilon\sigma}), \tag{11}$$

where

$$\mathbf{I}_{\varepsilon\sigma} = \begin{pmatrix} \varepsilon & 0 \\ 0 & \sigma \end{pmatrix}, \quad \mathbf{J}_{\varepsilon\sigma} = \begin{pmatrix} 0 & -\sigma \\ \varepsilon & 0 \end{pmatrix}. \tag{12}$$

4. MacKay's eigenvalue cones and instability bubbles

Modification of the stiffness matrix induced by the elastic support is typical in the models of computer disc drives [4], circular saws [7], disc brakes [9, 15, 21], and turbine discs [1, 16, 17]. Assuming $\delta = 0$ and $\nu = 0$ in (11) we find that the eigenvalues of the system (1) with the stiffness modification $\kappa\mathbf{K}$ either are pure imaginary and form a conical surface (Fig. 1(a)) in the $(\Omega, \kappa, \mathrm{Im}\lambda)$-space with the apex at the point $(\Omega_0, 0, \omega_0)$

$$\left(\mathrm{Im}\lambda - \omega_0 - \frac{\kappa}{8}\left(\frac{\mathrm{tr}\mathbf{K}_{ss}}{\alpha\omega_s} + \frac{\mathrm{tr}\mathbf{K}_{tt}}{\beta\omega_t}\right) - \frac{\Omega - \Omega_0}{2}(s\varepsilon + t\sigma)\right)^2 = \mathrm{Re}c, \tag{13}$$

or they are complex and in the $(\Omega, \kappa, \mathrm{Re}\lambda)$-space their real parts form a cone $(\mathrm{Re}\lambda)^2 = -\mathrm{Re}c$ with the apex at $(\Omega_0, 0, 0)$, Fig. 1(c), while the imaginary parts in the $(\Omega, \kappa, \mathrm{Im}\lambda)$-space are on the plane

$$\mathrm{Im}\lambda = \omega_0 + \frac{\kappa}{8}\left(\frac{\mathrm{tr}\mathbf{K}_{ss}}{\alpha\omega_s} + \frac{\mathrm{tr}\mathbf{K}_{tt}}{\beta\omega_t}\right) + \frac{\Omega - \Omega_0}{2}(s\varepsilon + t\sigma), \tag{14}$$

which is attached to the cone (13) as shown in Fig. 1(b). For $\alpha\beta < 0$ the cones $(\mathrm{Re}\lambda)^2 = -\mathrm{Re}c$ are near-horizontally oriented and extended along the κ-axis in the $(\Omega, \kappa, \mathrm{Re}\lambda)$-space with ellipses in their cross-sections by the planes $\kappa = const$, Fig. 1(c). Since at a part of the ellipse $\mathrm{Re}\lambda > 0$, it is called the *bubble of instability* [3]. Near the crossings with $\alpha\beta > 0$ the perturbed eigenvalues are pure imaginary (stability). The cones of imaginary parts (13) are then near-vertically oriented, Fig. 1(a). In the plane $\kappa = const$ this yields the *avoided crossing* [3], Fig. 1(a).

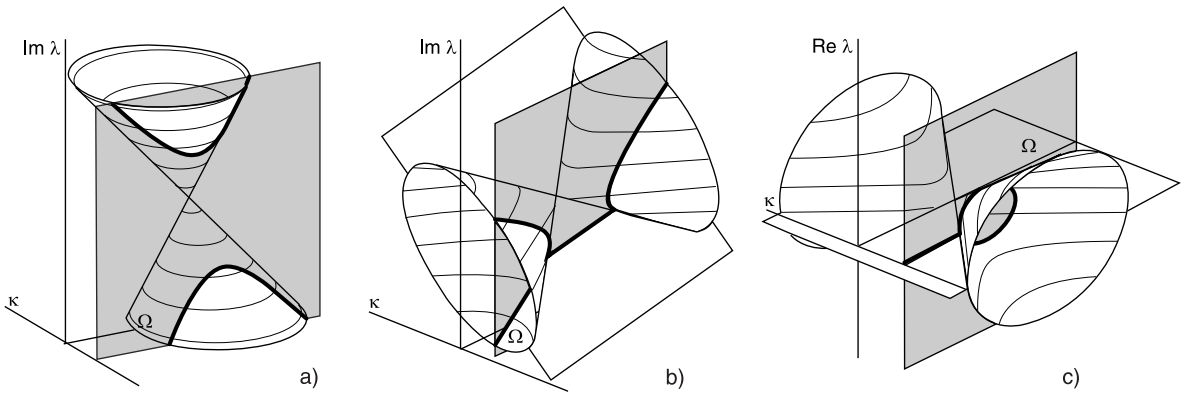

Figure 1. MacKay's eigenvalue cones [3] and (bold lines) their cross-sections in the plane $\kappa = const$ (grey): (a) in the subcritical range ($\mathrm{Re}\lambda = 0$); (b) , (c) in the supercritical speed range.

The sign of $\alpha\beta$ is negative only if the crossing in the Campbell diagram is formed by the eigenvalue branch of the reflected wave and by that of either forward- or backward traveling wave that occur only in the *supercritical* speed range ($|\Omega| \geq \Omega_{cr}$) due to the property $\omega_{s+1} - \omega_s \geq \Omega_s^{cr}$. Otherwise, $\alpha\beta > 0$. The crossings with $\alpha\beta > 0$ are situated in both the super- and *subcritical* ($|\Omega| < \Omega_{cr}$) ranges. Therefore, the eigenvalues with $\mathrm{Re}\,\lambda \neq 0$ originate only near the supercritical crossings with $\alpha\beta < 0$, when the parameters in the (Ω, κ)-plane are in the sector $\mathrm{Re}\,c < 0$.

The existence of the two different orientations of the eigenvalue cones in the Hamiltonian systems was established in [3]. This result goes back to Krein [2], who introduced the notion of the signature of eigenvalues in 1950s. To evaluate it we reduce (2) to the form $\dot{\mathbf{y}} = \mathbf{A}\mathbf{y}$, where

$$\mathbf{A} = \begin{pmatrix} -\Omega\mathbf{G} & \mathbf{I}_n \\ -\mathbf{P} & -\Omega\mathbf{G} \end{pmatrix} = \mathbf{J}_{2n}\mathbf{A}^T\mathbf{J}_{2n}, \quad \mathbf{J}_{2n} = \begin{pmatrix} 0 & -\mathbf{I}_n \\ \mathbf{I}_n & 0 \end{pmatrix}, \quad \mathbf{y} = \begin{pmatrix} \mathbf{x} \\ \dot{\mathbf{x}} + \Omega\mathbf{G}\mathbf{x} \end{pmatrix}. \tag{15}$$

The matrix $\mathbf{A}$ is self-adjoint in a Krein space with the indefinite inner product $[\mathbf{a}, \mathbf{b}] = \bar{\mathbf{b}}^T \mathbf{J}_{2n}\mathbf{a}, \quad \mathbf{a}, \mathbf{b} \in \mathbb{C}^{2n}$. It has the eigenvalues $\lambda_s^{\pm}$ (5) with the eigenvectors

$$\mathbf{a}_s^{++} = \begin{pmatrix} \mathbf{u}_s^+ \\ \lambda_s^+\mathbf{u}_s^+ + \Omega\mathbf{G}\mathbf{u}_s^+ \end{pmatrix}, \quad \mathbf{a}_s^{+-} = \begin{pmatrix} \mathbf{u}_s^- \\ \lambda_s^-\mathbf{u}_s^- + \Omega\mathbf{G}\mathbf{u}_s^- \end{pmatrix}. \tag{16}$$

Since $i[\mathbf{a}_s^{++}, \mathbf{a}_s^{++}] = i[\mathbf{a}_s^{+-}, \mathbf{a}_s^{+-}] = 4\omega_s > 0,$ the eigenvalues λ_s^+ and λ_s^- of the forward and backward traveling waves acquire *positive Krein signature*. The eigenvalues $\overline{\lambda_s^+}$ and $\overline{\lambda_s^-}$ of the reflected waves with $i[\mathbf{a}_s^{-+}, \mathbf{a}_s^{-+}] = i[\mathbf{a}_s^{--}, \mathbf{a}_s^{--}] = -4\omega_s < 0,$ have the *negative Krein signature*. This implies $\alpha\beta > 0$ and near-vertically oriented cones (14) at the crossings the *definite* Krein signature and $\alpha\beta < 0$ and near-horizontally oriented cones of imaginary parts (14) at the crossings with the *mixed* Krein signature [3]. The Krein signature coincides with the sign of the second derivative of the energy [3]. Interaction of waves with positive and negative energy is a well known mechanism of instability of the moving fluids and plasmas [3, 18]; in rotor dynamics this yields flutter in the supercritical speed range, which is known as the mass and stiffness instabilities [5, 9, 16, 19].

5. Double coffee filter singularity and definite Krein signature

In the high-speed rotor dynamical applications the *supercritical flutter* and *divergence* instabilities are easily excited near the crossings with the mixed Krein signature by the Hamiltonian perturbations only, which are not enough, however, to excite the *subcritical flutter* near the crossings with the definite Krein signature in the low-speed applications. In this case the non-Hamiltonian dissipative and circulatory forces are required for destabilization [9, 19].

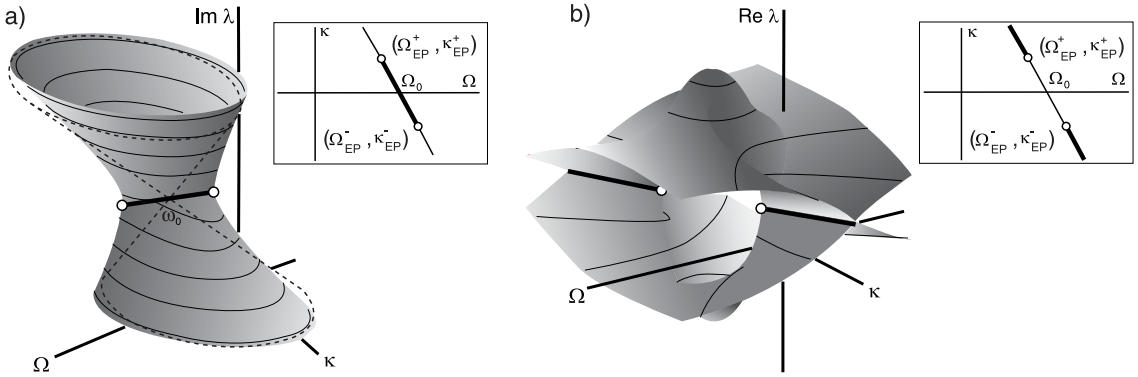

Figure 2. (a) The "double coffee filter" singular surface $\mathrm{Im}\lambda(\Omega,\kappa)$ with the exceptional points (open circles) and branch cut (bold lines) originated from the MacKay's cone (dashed lines) at any crossing with the definite Krein signature; (b) the corresponding "viaduct" singular surface $\mathrm{Re}\lambda(\Omega,\kappa)$.

The untwisting of the Campbell diagram in the subcritical speed range is directly related to the onset of friction-induced oscillations in brakes, clutches, paper calenders, and even in musical instruments like the glass harmonica [4, 5, 6, 7, 9, 14, 15, 19, 21].

In general, dissipative, $\delta\mathbf{D}$, and non-conservative, $\nu\mathbf{N}$, perturbations unfold the eigenvalue cones (14) and $(\mathrm{Re}\lambda)^2 = -\mathrm{Re}c$ into the surfaces $\mathrm{Im}\lambda(\Omega,\kappa)$ and $\mathrm{Re}\lambda(\Omega,\kappa)$, described by the formulas (9). The new eigenvalue surfaces have singularities at the *exceptional points* [11, 12], corresponding to the double eigenvalues with the Jordan chain that born from the double eigenvalue $i\omega_0$ at $\Omega = \Omega_0$. The condition $c = 0$ yields the loci of the exceptional points in the (Ω,κ)-plane

$$\Omega^{\pm}_{EP} = \Omega_0 \pm \frac{4\omega_s\omega_t U - \beta\omega_s \mathrm{tr}\mathbf{K}_{tt} + \alpha\omega_t \mathrm{tr}\mathbf{K}_{ss}}{4\omega_s\omega_t(t\sigma - s\varepsilon)}\sqrt{\frac{N}{D}},\ \kappa^{\pm}_{EP} = \pm\sqrt{\frac{N}{D}}, \tag{17}$$

where

$$U = \frac{\mathrm{Re}A_2 \mathrm{tr}\mathbf{K}_{st}\mathbf{J}_{\varepsilon\sigma} - \mathrm{Re}B_2 \mathrm{tr}\mathbf{K}_{st}\mathbf{I}_{\varepsilon\sigma}}{\alpha\omega_s \mathrm{Im}B_1 - \beta\omega_t \mathrm{Im}A_1}, \quad D = U^2 + \alpha\beta\left[\left(\frac{\mathrm{tr}\mathbf{K}_{st}\mathbf{J}_{\varepsilon\sigma}}{2\sqrt{\omega_s\omega_t}}\right)^2 + \left(\frac{\mathrm{tr}\mathbf{K}_{st}\mathbf{I}_{\varepsilon\sigma}}{2\sqrt{\omega_s\omega_t}}\right)^2\right],$$

$$N = \left(\frac{\alpha\omega_s \mathrm{Im}B_1 - \beta\omega_t \mathrm{Im}A_1}{4\omega_s\omega_t}\right)^2 + \alpha\beta\left[\left(\frac{\mathrm{Re}A_2}{2\sqrt{\omega_s\omega_t}}\right)^2 + \left(\frac{\mathrm{Re}B_2}{2\sqrt{\omega_s\omega_t}}\right)^2\right]. \tag{18}$$

The crossings with the definite Krein signature $(\alpha\beta > 0)$ always produce a pair of the exceptional points. The conditions for coincidence of imaginary parts of the eigenvalues (9) are $\mathrm{Im}c = 0$ and $\mathrm{Re}c \le 0$ and that for coincidence of the real parts are $\mathrm{Im}c = 0$ and $\mathrm{Re}c \ge 0$. Both real and imaginary parts coincide only at the exceptional points $(\Omega^+_{EP}, \kappa^+_{EP})$ and $(\Omega^-_{EP}, \kappa^-_{EP})$. The segment of the line $\mathrm{Im}c = 0$ connecting the exceptional points is the projection of the branch cut of a singular eigenvalue surface $\mathrm{Im}\lambda(\Omega,\kappa)$. The adjacent parts of the line correspond to the branch cuts of the singular eigenvalue surface $\mathrm{Re}\lambda(\Omega,\kappa)$. The surface of the imaginary parts $\mathrm{Im}\lambda(\Omega,\kappa)$ shown in Fig. 2(a) is formed by the two Whitney's umbrellas with the handles (branch cuts) glued when they are oriented toward each other. This singular surface is known in the literature on the wave propagation in anisotropic media as the double coffee filter [12]. The double coffee filter singularity is a result of the deformation of the MacKay's eigenvalue cone by the dissipative and non-conservative perturbations. These perturbations foliate the plane $\mathrm{Re}\lambda = 0$ into the viaduct singular surface of the real parts $\mathrm{Re}\lambda(\Omega,\kappa)$, which has self-intersections along the two branch cuts and an ellipse-shaped arch between the two exceptional points, Fig. 2(b). Structural modification of the matrices of dissipative and non-conservative forces generically does not change the type of the surfaces, preserving the exceptional points and the branch cuts.

6. A rotating circular string

Consider a circular string of displacement $W(\varphi,\tau)$, radius r, and mass per unit length ρ, that rotates with the speed γ and passes at $\varphi = 0$ through a massless eyelet [6]. The circumferential tension P in the string is constant; the stiffness of the spring supporting the eyelet is K and the damping coefficient of the viscous damper is D; the velocity of the string in the φ direction has constant value γr. With the non-dimensional variables and parameters

$$t = \frac{\tau}{r}\sqrt{\frac{P}{\rho}}, \quad w = \frac{W}{r}, \quad \Omega = \gamma r\sqrt{\frac{\rho}{P}}, \quad k = \frac{Kr}{P}, \quad d = \frac{D}{\sqrt{\rho P}} \tag{19}$$

substitution of $w(\varphi,t) = u(\varphi)\exp(\lambda t)$ into the governing equation and boundary conditions yields

$$Lu = \lambda^2 u + 2\Omega\lambda u' - (1-\Omega^2)u'' = 0, \quad u(0) - u(2\pi) = 0, \quad u'(0) - u'(2\pi) = \frac{\lambda d + k}{1-\Omega^2}u(0) \tag{20}$$

where $' = \partial_\varphi$. Without damping the eigenvalue problem (20) has the eigenvalues $\lambda_n^\varepsilon = in(1+\varepsilon\Omega)$ and $\lambda_m^\delta = im(1+\delta\Omega)$, where $\varepsilon,\delta = \pm 1$ and $n,m \in \mathbb{Z} - \{0\}$. In the $(\Omega, \mathrm{Im}\lambda)$-plane these eigenvalue branches intersect each other at the node (Ω_0, ω_0) with

$$\Omega_0 = \frac{n-m}{m\delta - n\varepsilon}, \quad \omega_0 = \frac{nm(\delta-\varepsilon)}{m\delta - n\varepsilon}, \tag{21}$$

where the double eigenvalue $\lambda_0 = i\omega_0$ has two linearly independent eigenfunctions

$$u_n^\varepsilon = \cos(n\varphi) - \varepsilon i\sin(n\varphi), \quad u_m^\delta = \cos(m\varphi) - \delta i\sin(m\varphi). \tag{22}$$

Intersections of the branch with $n = 1$ and $\varepsilon = 1$ and the branches with $m > 0$ and $\delta < 0$ in the subcritical range $(|\Omega| < 1)$ are marked in Fig. 3(a) by the red dots.

Taking into account that $\delta = -\varepsilon$ at all the crossings, excluding $(\Omega_0 = \pm 1, \omega_0 = 0)$ where $\delta = \varepsilon$, we find the real and imaginary parts of the dissipatively perturbed double eigenvalues

$$\mathrm{Re}\lambda = -\frac{d}{4\pi} \pm \sqrt{\frac{|c| - \mathrm{Re}c}{2}}, \quad \mathrm{Im}\lambda = \omega_0 + \varepsilon\frac{n-m}{2}\Delta\Omega + \frac{n+m}{8\pi nm}k \pm \sqrt{\frac{|c| + \mathrm{Re}c}{2}}, \tag{23}$$

where $\Delta\Omega = \Omega - \Omega_0$, and for the complex coefficient c we have

$$\mathrm{Im}c = k\frac{2d\omega_0}{16\pi^2 nm} + d\omega_0\frac{m-n}{4\pi nm}\left(\varepsilon\frac{n+m}{2}\Delta\Omega + \frac{m-n}{8\pi nm}k\right),$$

$$\mathrm{Re}c = \left(\frac{\varepsilon n - \delta m}{2}\Delta\Omega + \frac{m-n}{8\pi nm}k\right)^2 + \frac{k^2}{16\pi^2 nm} - \frac{\left[d(m+n)\omega_0\right]^2}{64\pi^2 n^2 m^2}. \tag{24}$$

Setting $\mathrm{Re}c = 0$ and $\mathrm{Im}c = 0$ we find that at the exceptional points

$$\Omega_{EP} = \Omega_0 \pm \frac{\varepsilon(m+n)d\omega_0}{8\pi nm\sqrt{nm}}, \; k_{EP} = \mp\frac{(m-n)d\omega_0}{2\sqrt{nm}}, \mathrm{Re}\,\lambda_{EP} = \frac{-d}{4\pi}, \mathrm{Im}\,\lambda_{EP} = \frac{2nm}{n+m} \pm \frac{d}{4\pi}\frac{n-m}{\sqrt{nm}}. \tag{25}$$

The existence of the exceptional points (25) depends on the Krein signature of the intersecting branches, that is on the sign of the product nm, where $n,m \in \mathbb{Z} - \{0\}$. In the case of the rotating string all the crossings in the subcritical speed range $(|\Omega| < 1)$ have definite Krein signature $(nm > 0)$. For those in the supercritical speed range $(|\Omega| > 1)$ it is mixed with $nm < 0$. In the (Ω, κ)-plane the exceptional points are situated on the line $\mathrm{Im}c = 0$, i.e.,

$$k = -2\pi\varepsilon\frac{m^2 - n^2}{m^2 + n^2}\Delta\Omega. \tag{26}$$

In Fig. 3(b) we show in the complex plane the exceptional points (25) for the damping coefficient $d = 0.3$. The red open circles correspond to the exceptional points born after the splitting of the *diabolical* [11, 12] crossings with $n = 1$ and $\varepsilon = 1$, which are shown in Fig. 3(a,b) by the red dots.

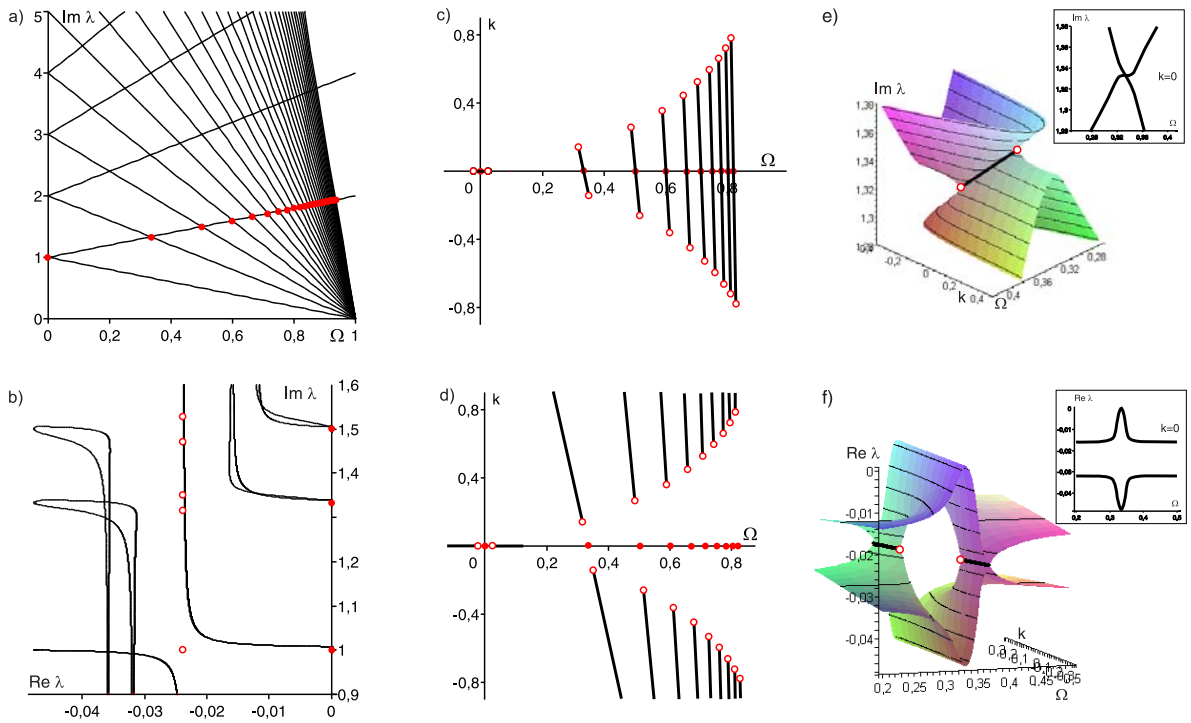

Figure 3. (a) The Campbell diagram of the unperturbed rotating string with red dots marking the nodes with $n = 1$; (b) a distribution of the exceptional points (open circles) born after the splitting of the diabolical points with $n = 1$ and $\varepsilon = 1$ in the complex plane when $d = 0.3$ and the trajectories of the eigenvalues $\lambda(\Omega)$ for $k = 0.05$; (c) projections of the branch cuts (26) of the coffee filters $\mathrm{Im}\lambda(\Omega, k)$ and the exceptional points for $n = 1$; (d) projections of the branch cuts (26) of the viaducts $\mathrm{Re}\lambda(\Omega, k)$ and the exceptional points for $n = 1$; (e) the double coffee filter singular surface $\mathrm{Im}\lambda(\Omega, k)$ and (f) the corresponding viaduct singular surface $\mathrm{Re}\lambda(\Omega, k)$ in the vicinity of the crossing with $n = 1$ and $m = 2$.

As it is seen in Fig. 3(b) the eigenvalue trajectories (9) make dramatic changes in the vicinity of the newborn exceptional poins, which qualitatively agrees with the numerical computations for particular mechanical models, see e.g. [15]. In Fig. 3(c) we plot the exceptional points originated after the splitting of the diabolical points together with the projections of the branch cuts (26) of the double coffee filters $\mathrm{Im}\lambda(\Omega, k)$. The corresponding projections of the branch cuts (26) of the viaducts $\mathrm{Re}\lambda(\Omega, k)$ are presented in Fig. 3(d). Only exceptional points descending from the doublets with $\Omega_0 = 0$ are situated on the Ω-axis. This explains why damping creates a perfect bubble of instability for the doublets with $m = n$ and imperfect ones for that with $m \neq n$ in accordance with [6]. Approximations (9) to the eigenvalue surfaces for a string with $d = 0.3$ are presented in Fig. 3(e,f). The smaller inclusions in Fig. 3 (e,f) show the cross-sections of the surfaces by the plane $k = 0$ that are in a good agreement with the numerical data of [6].

7. Conclusion

We found that in a weakly anisotropic rotor system (1) the branches of the Campbell diagram and the decay rate plots in the subcritical speed range are the cross-sections of the two companion singular eigenvalue surfaces. The double coffee filter and the viaduct are the imaginary and the real part of the unfolding of any double pure imaginary semi-simple eigenvalue at the crossing of the Campbell diagram with the definite Krein signature. Generically, the structure of the perturbing matrices does not yield the qualitative changes irrespective of whether the dissipative and circulatory perturbations are applied separately or in a mixture. The two eigenvalue surfaces found

unite seeming different problems on friction-induced instabilities in rotating elastic continua, because their existence does not depend on the specific model of the rotor-stator interaction and is dictated by the Krein signature of the eigenvalues of the isotropic rotor and by the dissipative and non-conservative nature of the forces originated at the frictional contact.

The work has been supported by the research grant DFG HA 1060/43-1.

REFERENCES

1. W. Campbell, The protection of steam-turbine disk wheels from axial vibration, *Trans. A.S.M.E.*, 1924, **46** 31-160.
2. M.G. Krein, Topics in Differential and Integral Equations and Operator Theory, Birkhauser, Basel, 1983.
3. R.S. MacKay, Stability of equilibria of Hamiltonian systems, In: *Nonlinear Phenomena and Chaos* (ed. S. Sarkar), Adam Hilger, Bristol, 1986, 254-270.
4. K. Ono, J.-S. Chen, D.B. Bogy, Stability analysis for the head-disk interface in a flexible disk drive, *Trans. ASME, J. Appl. Mech.*, 1991, **58**, 1005-1014.
5. J.E. Mottershead, S.N. Chan, Flutter instability of circular discs with frictional follower loads, *Trans. ASME, J. Vibr. Acoust.* **177**, 1995, 161-163.
6. L. Yang, S.G. Hutton, Interactions between an idealized rotating string and stationary constraints, *J. Sound Vibr.* **185**(1), 1995, 139-154.
7. J. Tian J., S.G. Hutton, Self-excited vibration in flexible rotating discs subjected to various transverse interactive forces: a general approach, *Trans. ASME. J. Appl. Mech.* **66**, 1999, 800.
8. A.L. Shuvalov, N.H. Scott, On singular features of acoustic wave propagation in weakly anisotropic thermoviscoelasticity, *Acta Mech.*, 2000, **140**, 1-15.
9. H. Ouyang, J.E. Mottershead, Unstable traveling waves in the friction-induced vibration of discs, *J. Sound Vibr.*, 2001, **248**(4), 768-779.
10. L.G. Xiong, H. Chen, J.M. Yi, Instability mechanism of a rotating disc subjected to various transverse interactive forces, *J. Mater. Proc. Techn.* **129** 2002, 534-538.
11. M.V. Berry, M.R. Dennis, The optical singularities of birefringent dichroic chiral crystals, *Proc. R. Soc. Lond. A*, 2003, **459**, 1261-1292.
12. F. Keck, H.-J. Korsch, S. Mossmann, Unfolding a diabolic point: a generalized crossing scenario, *J. Phys. A: Math. Gen*. **36,** 2003, 2125-2137.
13. O.N. Kirillov, A.A. Mailybaev, A.P. Seyranian, Unfolding of eigenvalue surfaces near a diabolic point due to a complex perturbation. *J. Phys. A: Math. Gen.* **38**(24), 2005, 5531-5546.
14. T.H. Young, C.Y. Lin, Stability of a spinning disk under a stationary oscillating unit, *J. Sound. Vibr.* **298**, 2006, 307-318.
15. J.-J. Sinou, F. Thouverez, L. Jezequel, Stability analysis and non-linear behaviour of structural systems using the complex non-linear modal analysis, *Comp. Struct.* **84** (2006) 1891.
16. G. Genta, Dynamics of rotating systems, Springer, 2007.
17. N. Lesaffre, J.-J. Sinou, F. Thouverez, Contact analysis of a flexible bladed-rotor, Eur. J. of Mech, - A/Solids, **26**(3) 2007, 541-557.
18. M. Hirota, Y. Fukumoto, Energy of hydrodynamic and magnetohydrodynamic waves with point and continuous spectra, *J. Math. Phys.* **49**(8), 2008, 083101.
19. O.N. Kirillov, Subcritical flutter in the acoustics of friction, *Proc. R. Soc. A*, **464**, 2008, 2321.
20. O.N. Kirillov, U. Gunther, F. Stefani, Determining role of Krein signature for three-dimensional Arnold tongues of oscillatory dynamos, *Phys. Rev. E.*, **79**(1), 2009, 016205.
21. G. Spelsberg-Korspeter, D. Hochlenert, O.N. Kirillov, P. Hagedorn, In- and out-of-plane vibrations of a rotating plate with frictional contact: Investigations on squeal phenomena, *Trans. ASME, J. Appl. Mech*. **76**(4), 2009, 041006.